



Synthesis and characterization of activated carbo-aluminosilicate material from oil shale

Reyad Awwad Shawabkeh *

Department of Chemical Engineering, Mutah University, Box 7, AL-Karak 61710, Jordan

Received 10 April 2004; received in revised form 5 June 2004; accepted 22 July 2004

Abstract

Three novel activated carbo-aluminosilicate materials were prepared from oil shale by chemical activation. The chemical used in the activation process were 95 wt% sulfuric acid and 5 wt% nitric acids to produce activated carbon (AC) supported on silica–alumina structure (ACASA), followed by treatment with either sodium hydroxide to produce AC within Na-type zeolite (ACASS) or by potassium hydroxides to obtain AC within K-type zeolite (ACASP). The specific surface areas of the three materials obtained using Sears' method were 314 m²/g for ACASA, 189 m²/g for ACASS and 292 m²/g for ACASP. X-ray diffraction analyses of these samples show the formation of zeolite Y, Na-X, and A-types, sodalite, sodium silicate, mullite and cancrinite. FT-IR spectrums show the presence of carboxylic, phenolic and lactonic groups on the surface of these samples. The total functional groups of these samples were measured using Boehm's method as: 5.02 mmol/g For ACASA, 2.91 mmol/g for ACASS and 4.08 mmol/g for ACASP. The corresponding cation exchange capacities were 146.9, 78 and 113.8 meq/100-g, respectively. Methylene blue adsorption by these adsorbent obtained at pH 7 show a multilayer of adsorption with saturation values of 117.9, 212.5 and 325.2 mg/g.

© 2004 Published by Elsevier Inc.

Keywords: Synthesis; Activated carbo-aluminosilicate; Adsorption; Oil shale; Characterization

1. Introduction

Activated carbon and zeolite are well known materials that are used extensively in industrial purification and chemical recovery operations. Activated carbon offers an attractive and inexpensive option for removal of several solutes from aqueous solutions. This AC has a specific affinity toward non-polar compounds such as organics. Due to its unique properties and stability in both acidic and basic media, activated carbon can also be used as a catalyst-support for different reactions. Zeolite, on the other hand, proved to be a good supportive material for several chemical engineering applications such as catalysis and ion exchange. Zeolite has a

hydrophilic affinity toward polar molecules as a result of existence of aluminum atoms in its structure.

Numerous researchers have focused on enhancing the physical and chemical properties of both activated carbon and zeolite [1–8]. These research areas focused either on surface modification, catalytic support, or utilization and finding new source of carbonaceous material. However, none of the above paid an attention for synthesizing a material that combine the physical and chemical properties of both activated carbon and zeolite.

Jordan reserves large quantity of oil shale. It is estimated that 50 billion ton of oil shale can be mined by open pit mining; while about 25–40% of this quantity can be extracted as oil [9]. The extraction process is costly and produces large quantity of ash. As a result, there is an alternative technology that makes use this

* Tel.: +962 6 461 7860; fax: +962 6 465 4061.

E-mail address: rshawabk@mutah.edu.jo (R.A. Shawabkeh).

natural material. This research focuses on conversion the carbonaceous materials and the ashes that exist in the oil shale into activated carbon and activated alumina and silica (activated carbo-aluminosilicate). The results relevant to this research are going to be presented in a series of papers that will cover major areas in activated carbo-aluminosilicate production from oil shale.

2. Experimental

2.1. Materials

Sodium and potassium hydroxide pellets (>98.5% purity), methylene blue and concentrated sulfuric and nitric acid were supplied by Sigma Chemical Company. Oil shale was collected from El-Lajjun area, AL-Karak County—Jordan. All solutions were prepared using deionized water from a Milli Q system (Millipore, France). All glassware were Pyrex washed with soap, rinsed with nitric acid the washed with deionized water.

2.2. Activation

Rocks of oil shale were collected, crushed and sieved to different particle sizes and stored for further treatment. Sample of 200 g of fine particles (<45 μm) was mixed with 400 ml of concentrated sulfuric (380 ml) and nitric acid (20 ml) solutions. The mixture is then heated to 270 °C while stirred using glass rod. Meanwhile, air is sparged into the solution with flow rate of 1.0 l/min to enhance the oxidation of the mixture. Once the solution get solidify, this solid material was cooled down at room temperature then washed with deionized water to remove any adhered acids. Then, the activated material was divided into three equal parts; one part left as is (ACASA), the second part is mixed overnight with 100 ml of 1.0 M sodium hydroxide (ACASS) while the third one is similarly treated as in the second part but with potassium hydroxide (ACASP).

3. Analysis and characterization

3.1. Fourier transform infrared spectroscopy

The surface functional groups of the activated carbo-aluminosilicate samples were analyzed by Fourier transform infrared spectrophotometry (FT-IR) using Shimadzu FTIR-8400S. Sample of 3.0 mg was mixed thoroughly with 1.0 g of fine dried powder of KBr. The resulting mixture was hydraulically pressed at 10^4 kg/m^2 to obtain a thin transparent disk. The thin disk was placed in an oven at 105 °C for 4 h to prevent any interference of any existing water vapor or carbon dioxide molecules.

3.2. X-ray diffraction measurements

X-ray diffraction spectroscopy (XRD) analyses were carried out with PANalytical X-ray, Philips Analytical. A dried sample of the produced material is grinded using an agat mortar and pestle and tested at 40 kV and 40 mA. The spectra were analyzed using PC-APD diffraction software.

3.3. Nuclear magnetic resonance spectroscopy

The NMR spectra were recorded at temperature of 298 K and at magnetic fields of 200 MHz for ^1H nuclei using Bruker spectrophotometer. Data processing was achieved with a SGi computer using XWin NMR software version 2.6. Samples (50 mg/0.8 ml) were dissolved in deuterated dimethylsulfoxide, and the solvent signal was used for spectral calibration (1 H: 2.49 mg/l). Proton spectra were run using the standard pulse sequence program 'zg' for recording 1D experiments.

3.4. Cation exchange capacity

Cation exchange capacity (CEC) was determined using sodium acetate procedure (SW-846 Method 9080) [10]. Sample of 4.0 g of the activated carbo-aluminosilicate was soaked with excess amount of 1.0 M sodium acetate solution, centrifuged and rinsed by isopropyl alcohol. Then a solution of ammonium acetate (1.0 M) was added to replace the amount of sodium adsorbed on the surface of the solid. The concentration of the displaced sodium was then determined using SOLAAR S4 atomic absorption spectrophotometer.

3.5. Surface area measurement

The surface area was estimated according to Sears' method for silica-based materials [11]. This can be obtained by agitating 1.5 g of each of the produced sample in 100 ml of diluted hydrochloric acid (pH 3). Then a 30 g of sodium chloride was added with stirring and the volume was made up to 150 ml with deionized water. The solution was titrated with 0.10 M NaOH and the volume, V , needed to raise the pH from 4 to 9 was then recorded.

3.6. Determination of the functional groups

The surface functional groups were determined using Boehm's titration procedure [12,13]. One hundred milligram of activated carbo-aluminosilicate was placed in 25 ml of 0.1 M solution of each of sodium bicarbonate, sodium carbonate or sodium hydroxide. The solid-solution mixtures were shaken for 24 h then centrifuged at 6000 rpm. A given amount of the each supernatant (5 ml) was back titrated with 0.1 M hydrochloric acid

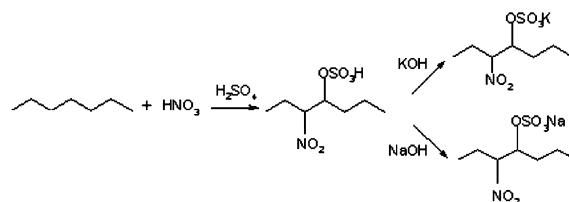
solution. Similar procedures were performed with blank samples. The number of acidic sites was determined under the assumptions that sodium bicarbonate neutralizes carboxylic groups, sodium carbonate neutralizes both carboxylic and lactonic groups and sodium hydroxide neutralizes carboxylic, lactonic and phenolic groups.

3.7. Methylene blue adsorption

Various concentrations of methylene blue solutions ranging from 25 to 350 mg/l were prepared by dissolving methylene blue crystals in deionized water and diluted to the required concentration. Adsorption isotherm was obtained by adding 0.1 g of activated carbo-aluminosilicate sample to 100 ml of each aqueous solution of methylene blue. The solid-solution samples were agitated in an isothermal shaker ($22 \pm 1^\circ\text{C}$) for 24 h. The suspension was then allowed to settle, and the concentration of the methylene blue was determined using Shimadzu UV-1601 Spectrophotometer at maximum wavelength of 646 nm.

4. Results and discussion

The chemical analysis of El-Lajjun oil shale shows it contains by weight 55% ash, 15% carbon, 4% water, and the rest are volatile matter. The ash content of this oil shale is presented in Table 1. The oil shale samples were treated with both sulfuric and nitric acids. The activation was performed by addition the sulfuric acid to the shale samples at room temperature where no effect was noticed on the mixture. Then the nitric acid was added gradually to the mixture, which resulted in a rapid increase in the solution temperature to 150°C reached within 1 min as a result of exothermic reaction. Then the solution was heated further while carbon monoxide, carbon and sulfur dioxide, and nitrous oxide were released out of the solution [14]. Upon activation with these acids, several sulfonation and nitrification reactions took place at the surface of the oil shale samples yielding an activated carbon with large surface functional groups according Scheme 1 [15,16].



Scheme 1. Proposed chemical reaction of surface of oil shale with the activation agents.

Also, treatment with the acids changed the composition of the ash in the sample where a chemical reaction took place between the calcium ions in the lime and the sulfate and nitrate in the acidic solution leading to the formation of calcium sulfate and nitrate. This could be leached out of the solid matrix during washing which leaving a skeleton with macro and micropores of alumina and silica as in ACASA. Further treatment of this alumina and silica-based solid material with sodium or potassium hydroxide allows further reaction on the surface of the produced activate carbon and cross-linked silica and alumina structures to form zeolite materials of ACASS and ACASP, respectively. El-Hendawy showed that treatment of activated carbon with nitric acid promotes hydrophilicity of the carbon surface [17]. While Lozano-Castelló et al. indicated that activation with sodium hydroxide can increase the surface area of the activated carbon and provides more micropores [18]. Moreover, Shawabkeh et al. showed that reaction of oil shale ash with sodium hydroxide would lead to the formation of zeolite at moderate temperature [19].

FT-IR spectroscopic studies for the three activated solid materials are shown in Fig. 1. All samples showed three major absorption bands at $3300\text{--}3600$, $1400\text{--}1700$ and $1050\text{--}1200\text{ cm}^{-1}$. ACASA showed a wide band with two maximum peaks at 3420 and 3566 cm^{-1} . This band can be assigned to the O—H stretching mode of hydroxyl groups and adsorbed water. Moreover, this broad peak band in the range of $3200\text{--}3650\text{ cm}^{-1}$ is attributed to the hydrogen-bonded OH group of alcohols and phenols [20,21]. The absorbance intensity for this peak was increase to about 150% of the original value when this sample was further treated with either sodium or potassium hydroxides as shown in ACASS and ACASP spectra. This is attributed to the changing of C—O bonds to carboxyl groups by the treatment with either potassium or sodium hydroxides.

In the $1050\text{--}1200\text{ cm}^{-1}$ regions, peaks at 1120 and 1155 cm^{-1} might be related to the carbon–oxygen dingle bonds displayed stretching in acids, phenols, ethers and esters [21]. Upon treatment with hydroxides, the absorption intensity of this band reduced to 35% with a shift to 1093 and 1101 cm^{-1} for both ACASS and ACASP, respectively, while peak at 1155 completely disappeared. This might be related to metal carbonation and metal

Table 1
Mass fraction of metal oxides in El-Lajjun oil shale ash

Component	Wt%
SiO ₂	27.5
Al ₂ O ₃	4.8
Fe ₂ O ₃	2.2
P ₂ O ₅	4.1
CaO	58.3
MgO	2.6
TiO ₂	0.36
Na ₂ O	0.14

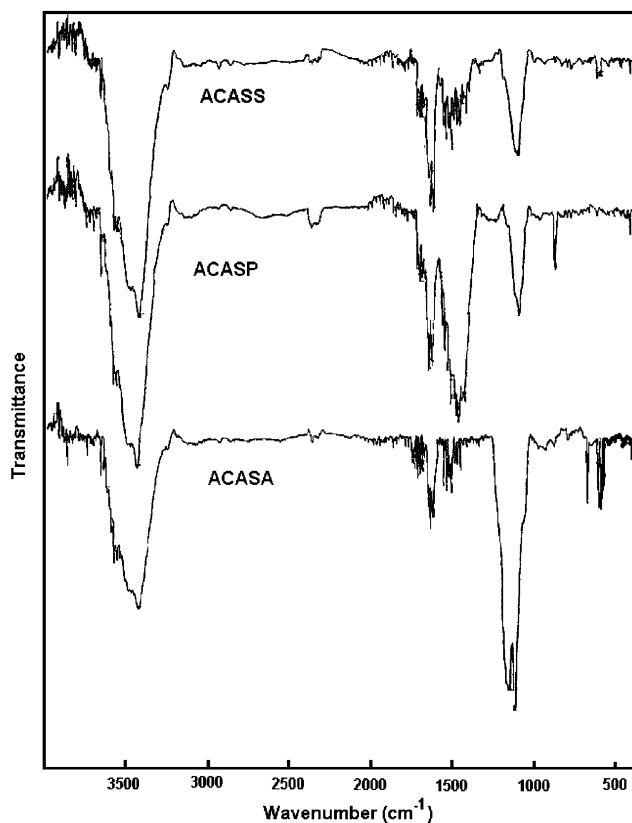


Fig. 1. FT-IR spectrum of activated carbo-aluminosilicate samples.

salt vibrational modes [22]. Moreover, the decrease of this peaks means that some of the functional group was removed as CO_2 to the gas phase or conversion to other functional group [23].

In the region $500\text{--}900\text{cm}^{-1}$, the ACASA shows two peaks at 594 and 680cm^{-1} . These peaks are assigned to the out-of-plane C—H bending mode. After treatment with sodium hydroxide these peaks were diminished and a new small peak appeared at 603cm^{-1} . Similarly, when further treatment with potassium hydroxide; a new peak at 875cm^{-1} was appeared as a result of C—H out-of-plane bending in benzene derivative. These spectra were suggested to be due to alkaline groups of cyclic ketons and its derivatives [22,24].

The peak at 1507cm^{-1} appeared in ACASA is due to C=C stretch in aromatic rings [24]. The intensity of this peak increased abruptly and shifted to 1456cm^{-1} when this carbo-aluminosilicate is further treated with potassium hydroxide. Similar peak appeared for the same sample treated with sodium hydroxide but with less intensity as for that treated with KOH. The peaks at $1600\text{--}1700\text{cm}^{-1}$ are due to the double bond C=O stretching vibrations with aromatic carbons [25,26]. ACASA displayed a peak at 1618cm^{-1} . This peak increased and shifted to 1637 and 1699cm^{-1} when this sample was treated with KOH. Similar behavior was obtained when it is treated with NaOH while it kept at

1616cm^{-1} . The absorption peak near 1699cm^{-1} is attributed to carboxylic group appeared as oxidation by nitric acid followed by either hydroxide treatment [23]. The band at 2343cm^{-1} is ascribed to the carbon-carbon triple bond vibrations in alkyne group [20]. The shoulders observed at this band are usually ascribed to the presence of aliphatic compounds [17].

X-ray diffractograms for the three carbo-aluminosilicates are shown in Fig. 2. The XRD spectra of these samples illustrated the presence of mullite, sodalite, quartz, and zeolite. ACASA demonstrated the presence of zeolite Y-type at $29^\circ 2\theta$ with relative intensity of 100% followed by zeolite Na-X type detected at 26° and $31^\circ 2\theta$. Other peaks were located at 36° and $45^\circ 2\theta$ for zeolite A, while the rest of the peaks for mullite, cancrinite, sodalite, or sodium silicates. When this sample is further treated with sodium hydroxide new peaks appeared as a result of formation of quartz at $21^\circ 2\theta$, hydroxyl-sodalite at $24^\circ 2\theta$ and zeolite A at $27^\circ 2\theta$. However, the peak appeared for zeolite Y in ACASA diffractograms was shifted to $31^\circ 2\theta$ and changed to zeolite Na-X in ACASS. On the other hand, the treatment with potassium hydroxide produced new zeolite Na-X obtained at $10^\circ 2\theta$ while two peaks with equal relative intensity appeared at 31° and $33^\circ 2\theta$ for zeolite R and mullite, respectively. When treating by either sodium hydroxide or potassium hydroxide there is a new quartz peak appeared at around $21^\circ 2\theta$ in both diffractograms.

The ^1H NMR spectra were recorded for the three carbo-aluminosilicate samples from 0 to 6 mg/l (Figs. 3 and 4). The three samples show two identical peaks at 0 and 2.3 mg/l. On the other hand, ACASA spectrum shows a major single peak at 4.2 mg/l as shown in Fig. 3, while both ACASS and ACASP spectra show an identical peak at 3.4 mg/l (Fig. 4). This shift from 4.2 to 3.4 was happened as a result of activation with either of sodium or potassium hydroxide. The peak at 2.3 mg/l is as a result of silanol groups and the one at 4.2 mg/l is attributed to resonance of hydrous $\text{NaAlSi}_3\text{O}_8$ crystal where a bridging of hydroxyl groups occurs [27]. In contrast, the peak that is appeared at 3.4 mg/l is attributed to the molecular H_2O resonance for hydrous $\text{Na}_2\text{Si}_4\text{O}_9$ crystal [28]. Upon alkali activation each Si—O(H)—Al unit in this structure is associated with one NaOH group. The “NaOH” resonance cannot be assigned to the 3.5 mg/l resonance. However, the assignment of this resonance to Si—OH groups is consistent with Si—O—Al or Si—O—Si bond breakage discussed by several researchers [28].

Since not all carbo-aluminosilicate particles are identical in size, the physical adsorption of nitrogen by these samples at 77 K is the best for prediction the surface area. However, the estimation of their surface area by titration method provides a rapid and relatively accurate number for their surface area. The surface area was obtained using Sears' method according to Eq. (1) as

$$S \text{ (m}^2\text{/g)} = 32V - 25 \quad (1)$$

where V is the volume of sodium hydroxide require raising the pH of the sample from 4 to 9. The obtained volume of sodium hydroxide solutions were 10.6, 6.7, 9.9 ml for ACASA, ACASS and ACASP, respectively. The corresponding surface areas calculated from the above equation are 314 m²/g for ACASA, 189 m²/g for ACASS and 292 m²/g for ACASP. The specific surface area of the ACASA is decreased by the chemical activation with either sodium or potassium hydroxides. This could be due to blocking of the narrow pores by the surface complexes introduced by further chemical treatment where the decrease of surface area was mainly ascribed to the decrease of the micropores volume [16].

Various studies on surface functional groups of adsorbents are already described in literature [22,24,26]. The change in surface acidity developed from sulfuric/nitric acid and sodium/potassium hydroxide treatment was detected by Boehm's titration measurement. For ACASA the total oxygen containing functional group is 5.02 mmol/g with a percentage of 53.8, 10.4, 35.8 for phenolic (–OH), lactone (C=O), and carboxylic (COOH) groups, respectively. Treatment with sodium hydroxide or potassium hydroxide decreased the total concentration of the oxygen containing functional group to 2.91 and 4.08 mmol/g, respectively. The percentage of the functional groups in ACASA were 54.02 for phenolic, 12.85 for lactonic and 33.13 for carboxylic groups. Similarly, the corresponding functional groups for ACASP sample were 54.11, 11.83 and 34.96 mmol/g in that order.

Treatment by sulfuric and nitric acids produces large amount of acidic surface groups which leads to an increase in the amount of bases required to neutralizing the oxidized material. On the other hand, the sodium and potassium hydroxide treatment resulted in a decrease of carboxyl surface groups [24]. Furthermore, the surface area and pore volume were decreased with the high concentration of NaOH or KOH. This was possibly due to the decomposing of excessive NaOH and KOH molecules into water, which thence dissolve the carbon content in the carbo-aluminosilicate material and blocked the micropores. This was cleared during the washing of the carbo-aluminosilicate with water after the treatment with concentrated bases where a dark pink color was appeared with the filtrate.

To further check the density of these functional groups on the surface of these samples, the cation exchange capacity was measured and shown in Fig. 5. It is appeared that ACASA shows the highest CEC while ACASS proved the lowest value.

Methylene blue was chosen in this study because of its known strong adsorption onto solids and its recognized usefulness in characterizing adsorptive material [29–31]. The isotherm results for the three carbo-alu-

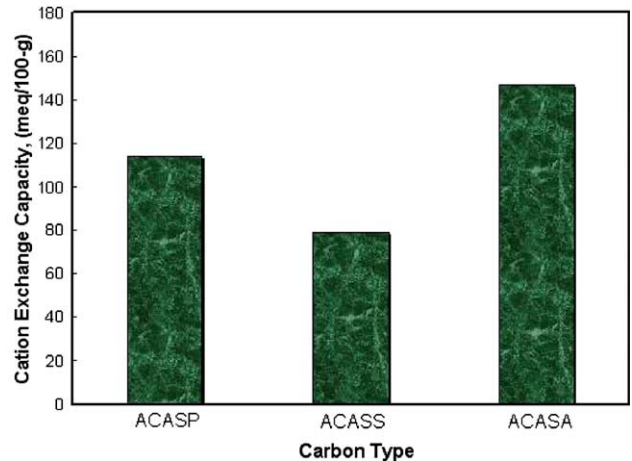


Fig. 5. Cation exchange capacity of activated carbo-aluminosilicate samples.

minosilicate samples obtained at pH 7 are presented in Fig. 6. It is clear that a multilayer of adsorption took place at the surface of these samples. These equilibrium data were fitted according to Langmuir model as in Eq. (2):

$$q_e = \frac{QbC_e}{1 + bC_e} \quad (2)$$

where C_e (mg/l) and q_e (mg/g) are the equilibrium concentrations in liquid and solid phases, respectively. Q (mg/g) is the maximum amount of methylene blue that can be adsorbed per unit mass of adsorbent to form a complete monolayer and b (l/mg) is the Langmuir constant that is related to the affinity of binding sites. Brunauer, Emmett and Teller (BET) model was also considered to fit these data (Eq. (3)), which assumes that a number of layers of adsorbate molecules form at the

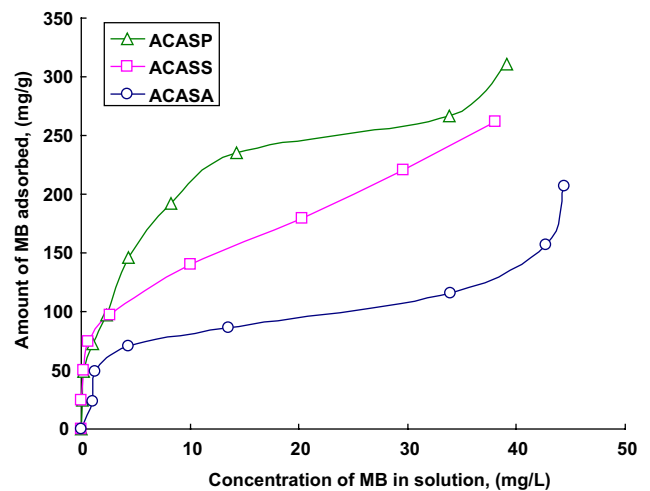


Fig. 6. Adsorption isotherms for the activated carbo-aluminosilicate samples.

Table 2
Parameters of adsorption isotherm of methylene blue onto activated carbo-aluminosilicate samples

Material type	Langmuir model			BET model			
	Q	b	R^2	Q	k_1	k_m	R^2
ACASA	117.9	0.342	0.957	64.2	1.273	0.015	0.960
ACASS	212.6	0.437	0.911	132.9	2.268	0.011	0.971
ACASP	324.2	0.198	0.975	233.1	0.390	0.007	0.981

surface of adsorbent and that the Langmuir equation, is applied to each layer of adsorption thus:

$$q_e = \frac{Qk_1C_e}{(1 - k_mC_e)[1 + (k_1 - k_m)C_e]} \quad (3)$$

where k_1 and k_m are the equilibrium constants for the first and subsequent layers, respectively. The other parameters are the same as in Eq. (2). The corresponding isotherm constants are presented in Table 2, which show that the ACASA has a maximum uptake of 117.9 mg/g, ACASS showed an uptake of 212.5 mg/g while ACASP showed an uptake capacity of 325.2 mg/g. When comparing the cation exchange capacity for these samples the increase in the adsorption capacities should be in the order of ACASA, ACASP and ACASS. The reason behind this difference in finding between the CEC values and the maximum uptake for methylene blue could be attribute to the fact that adsorption of methylene blue is enhanced not only by the exchangeable sites but also by the availability of surface area where multilayers can be formed. Moreover, methylene blue has a hydrophobic inorganic part which directed to adsorption by the surface both activated carbon and zeolite. Also activation with sodium and potassium hydroxides decreased the particle diameter of the carbo-aluminosilicate samples and hence increased the surface area per unit mass. This was observed when the supernatant solution after activation was filtered, a brownish color was observed and the pressure drop on the filter was increased and hence blocked the filter. This decrease in the solid particles leads to a very fine ones, which increase the available surface area of the whole sample and as a result increases the methylene blue adsorption.

5. Conclusion

Synthesis and production of activated carbon and zeolite from oil shale can lead providing an adsorbent material with high affinity toward removal of both organic and inorganic solute from wastewater. This material can be utilized in heterogeneous chemical reactions as a supporting catalyst. It can tolerate compression and high temperature.

Acknowledgments

The author would like to acknowledge the Deanship of Research at Mutah University and the Higher Council for Scientific Research at Royal Scientific Society-Jordan for their financial support to this research.

References

- [1] Z. Lin, J. Rocha, A. Ferreira, M. Anderson, *Colloids and Surfaces A: Physicochemical and Engineering Aspects* 179 (2001) 133.
- [2] Y. Chang, D. Wang, T. Wu, *Thin Solid Films* 420–421 (2002) 241.
- [3] Y. Kim, K. Choi, *Sensors and Actuators B: Chemical* 87 (2002) 196.
- [4] R. Shawabkeh, D. Rockstraw, R. Bhada, United States Patent number 6,225,256.
- [5] P. Parmentier, J. Joly, A. Perrard, United States Patent number 6,383,972.
- [6] Y. Xia, R. Mokaya, *Microporous and Mesoporous Materials* 62 (2004) 1.
- [7] G. Mehos, H. Tu, United States Patent number 6,541,113.
- [8] C. Zhang, Q. Liu, Z. Xu, K. Wan, *Microporous and Mesoporous Materials* 62 (2003) 157.
- [9] National Energy Research Center, Hashemite Kingdom of Jordan, Report 1, Royal Scientific Society, Amman, Jordan.
- [10] United States Environmental Protection Agency, <http://www.epa.gov/>.
- [11] G. Sears, *Analytical Chemistry* 28 (1956) 1981.
- [12] Y. Li, S. Wang, Z. Luan, J. Ding, C. Xu, W. Wu, *Carbon* 41 (2003) 1057.
- [13] H. Boehm, *Carbon* 40 (2002) 145.
- [14] I. Mochida, S. Kawano, *Industrial and Engineering Chemistry Research* 30 (1991) 2322.
- [15] E. Dimotakis, M. Cal, J. Economy, M. Rood, S. Larson, *Environmental Science and Technology* 29 (1995) 1876.
- [16] K. Benak, L. Dominguez, J. Economy, C. Mangun, *Carbon* 40 (2002) 2323.
- [17] A. El-Hendawy, *Carbon* 41 (2003) 713.
- [18] D. Lozano-Castelló, A. Lillo-Ródenas, D. Cazorla-Amorós, A. Linares-Solano, *Carbon* 39 (2001) 741.
- [19] R. Shawabkeh, A. Harahsheh, M. Hami, A. Khlaifat, *Fuel* 83 (2004) 981.
- [20] T. Yang, A. Lua, *Journal of Colloid and Interface Science* 267 (2003) 408–417.
- [21] A. Puziy, O. Poddubnaya, A. Martínez-Alonso, F. Suárez-García, J. Tascón, *Carbon* 41 (2003) 1181.
- [22] S. Park, S. McClain, Z. Tian, S. Suib, C. Karwacki, *Chemistry of Materials* 9 (1997) 176.
- [23] S. Shin, J. Jang, S. Yoon, I. Mochida, *Carbon* 35 (1997) 1739.

- [24] J. Guo, A. Lua, *Microporous and Mesoporous Materials* 32 (1999) 111.
- [25] R. Arriagada, R. Garcia, M. Molina-Sabio, F. Rodriguez-Reinoso, *Microporous Materials* 8 (1997) 123.
- [26] H. Chiang, C. Huang, P. Chiang, *Chemosphere* 47 (2002) 257.
- [27] D. Freude, *Chemical Physics Letter* 235 (1995) 69.
- [28] Q. Zeng, H. Nekvasil, C. Grey, *Journal of Physical Chemistry B* 103 (1999) 7406.
- [29] M. Froix, R. Nelson, *Macromolecules* 8 (1975) 726.
- [30] S. Barton, *Carbon* 25 (1987) 343.
- [31] Z. Shappley, J. Jenkins, J. Zhu, J. McCarty, *The Journal of Cotton Science* 2 (1998) 153.